Inevitable global coral reef decline under climate change-induced thermal stresses

Kai Zeng[1,2], Song He[3,4], and Peng Zhan [1*]

[1] *Department of Ocean Science and Engineering, Southern University of Science and Technology, Shenzhen, China.*

[2] *Donghai Laboratory, Zhoushan, China.*

[3] *Red Sea Research Center, King Abdullah University of Science and Technology (KAUST), Thuwal, Saudi Arabia.*

[4] *KAUST Beacon Development, KAUST National Transformation Institute, Innovation Cluster, King Abdullah University of Science and Technology (KAUST), Thuwal, Saudi Arabia.*

***Corresponding Author：** Peng Zhan (zhanp@sustech.edu.cn)

Summary: fifteen pages, three tables, seven figures.

Table of Contents

The Supplementary information is organized as follows:

6. Figure S3. Diagnostic analysis of model uncertainty based on random forest prediction variance.

7. Figure S4. Models of 10 random forest training based on the global coral-bleaching database.

8. Figure S5. Standard diagnostic plots for the linear regression between coral reef decline rate (%) and bleaching severity across 10 tropical ocean regions.

9. Figure S6. Standard deviation of mean annual coral bleaching projections based on CMIP6 data for the periods 2020–2060 (a, c, and e) and 2060–2100 (b, d, and f), under three climate scenarios: high emission pattern SSP5-8.5 (e and f), medium emission pattern SSP2-4.5 (c and d), and low emission pattern SSP1-2.6 (a and b).

10. Figure S7. Projected coral decline under three climate scenarios: (a, b) low emission (SSP1-2.6), (c, d) medium emission (SSP2-4.5), and (e, f) high emission (SSP5-8.5) during the periods 2020–2060 (a, c, e) and 2060–2100 (b, d, f).

Supplementary Table 1. Average live hard coral cover from GCRMN status of coral reefs of the world: 2020 report

Region	Coverage in 1979	Coverage in 2019	Decline
East Asian Seas	32.50%	36.79%	-4.29%
Caribbean	18.08%	15.9%	2.18%
Australia	35.17%	26.05%	9.12%
Brazil	20.39%	20.59%	-0.20%
West Indian Ocean	26.43%	29.37%	-2.94%
South Asia	46.36%	23.33%	23.03%
Red Sea and the Gulf of Aden	36.75%	34.28%	2.47%
Pacific	37.03%	31.35%	5.68%
East Tropical Pacific	36.87%	22.83%	14.04%
The Gulf and Gulf of Oman	30.85%	17.93%	12.92%
Global	32.30%	29.52%	2.78%

Supplementary Table 2. Information on CMIP6 Models. 17 CMIP6 models were evaluated, and here we focus on the projected temperature-related variables from three Representative Concentration Pathways emission scenarios: SSP1-2.6, SSP2-4.5, and SSP5-8.5.

Model	Nominal resolution	Total levels (ocean)	Top grid thickness (ocean)	References
ACCESS-CM2	250 km	50	10 m	Dix et al., 2019
ACCESS-ESM1-5	250 km	50	10 m	Ziehn et al., 2019
BCC-CSM2-MR	100 km	40	10 m	Xin et al., 2019
CanESM5	100 km	45	6 m	Swart et al., 2019
CESM2-WACCM	100 km	60	10 m	Danabasoglu, 2019
CMCC-CM2-SR5	100 km	50	1 m	Lovato et al., 2020
CMCC-ESM2	100 km	50	1 m	Lovato et al., 2021
EC-Earth3	100 km	75	1 m	EC-Earth Consortium, 2019
EC-Earth3-Veg	100 km	75	1 m	EC-Earth Consortium, 2019
EC-Earth3-Veg-LR	100 km	75	1 m	EC-Earth Consortium, 2020
IPSL-CM6A-LR	100 km	75	2 m	Boucher et al., 2019
MIROC6	100 km	63	2 m	Shiogama et al., 2019
MPI-ESM1-2-HR	50 km	40	12 m	Schupfner et al., 2019
MRI-ESM2-0	100 km	61	2 m	Yukimoto et al., 2019
NESM3	100 km	46	6 m	Cao, 2019
NorESM2-LM	100 km	70	2.5 m	Seland et al., 2019
NorESM2-MM	100 km	70	2.5 m	Bentsen et al., 2019

Supplementary Table 3. Environmental Variables for Random Forest Model Training

Variables	Meaning	Units
Latitude	Latitude coordinates in decimal degrees.	degree
Longitude	Longitude coordinates in decimal degrees.	degree
Depth	Water depth.	m
Windspeed	Marine wind speed.	m/s
Temp	Sea surface temperature (SST) in Kelvin.	K
Temp _min	The minimum weekly SST over the entire period.	K
Temp _max	The maximum weekly SST over the entire period.	K
Temp _SD	Standard deviation of weekly SST over the entire period.	K
ClimSST	Weekly climatological SST	K
SSTA	Weekly SST minus weekly climatological SST	°C
SSTA_min	The minimum weekly SSTA over the entire period.	°C
SSTA_max	The maximum weekly SSTA over the entire period.	°C
SSTA_SD	Standard deviation of SSTA over the entire period.	°C
SSTA_Frequency	Number of times over previous 52 weeks that SSTA is greater than or equal to 1 degree C	-
SSTA_Frequency_SD	Standard deviation of SSTA_Frequency over the entire period.	-
SSTA_Frequency_max	The maximum weekly SSTA_Frequency over the entire period.	-
SSTA_DHW	Sum of previous 12 weeks when SSTA is greater than or equal to 1 degree C	Weekly °C

SSTA_DHW_SD	Standard deviation of SSTA_DHW over the entire period.	Weekly °C
SSTA_DHW_max	The maximum weekly SSTA_DHW over the entire period.	Weekly °C
TSA	Weekly SST minus the maximum weekly climatological SST	°C
TSA_min	The minimum weekly TSA over the entire period.	°C
TSA_max	The maximum weekly TSA over the entire period.	°C
TSA_SD	Standard deviation of TSA over the entire period.	°C
TSA_Frequency	Number of times over previous 52 weeks that TSA is greater than or equal to 1 degree C	-
TSA_Frequency_SD	Standard deviation of TSA_Frequency over the entire period.	-
TSA_Frequency_max	The maximum weekly TSA_Frequency over the entire period.	-
TSA_DHW	Sum of previous 12 weeks when TSA is greater than or equal to 1 degree C	Weekly °C
TSA_DHW_SD	Standard deviation of TSA_DHW over the entire period.	Weekly °C
TSA_DHW_max	The maximum weekly TSA_DHW over the entire period.	Weekly °C
Turbidity	In terms of the downwelling diffuse attenuation coefficient of 490 nm ($K_d(490)$)	m^{-1}
Distance_to_Shore	The distance of the sampling site from the nearest land.	m
Cyclone_Frequency	Number of cyclone events from 1964 to 2014.	-

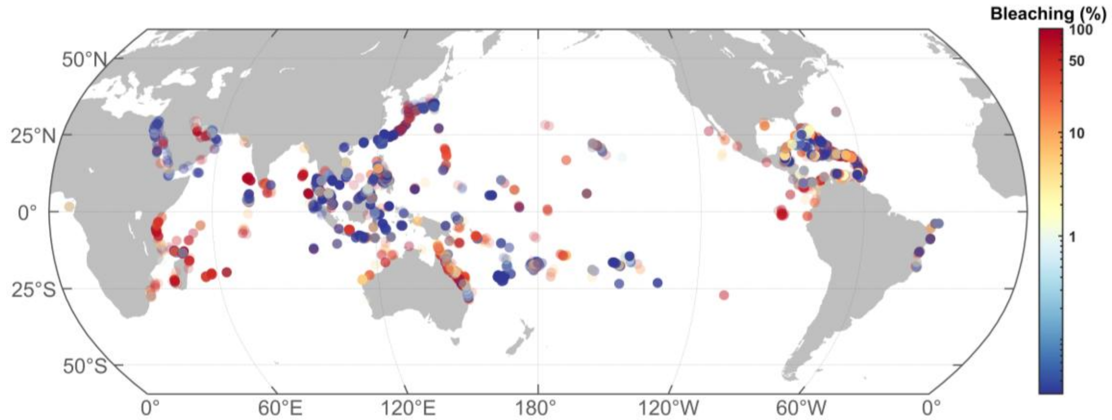

Figure S1. Spatial distribution of coral bleaching records from 1980 to 2020, based on 34,846 individual observations from 14,405 sites in 93 countries. Each dot represents a single field survey record, including both presence and absence of bleaching, as compiled in the global coral bleaching database (van Woesik & Kratochwill, 2022). Spatial autocorrelation was assessed using Moran's I based on site coordinates. A Moran's I of 0.26 indicated moderate positive spatial autocorrelation, typical in ecological datasets and not expected to bias model performance.

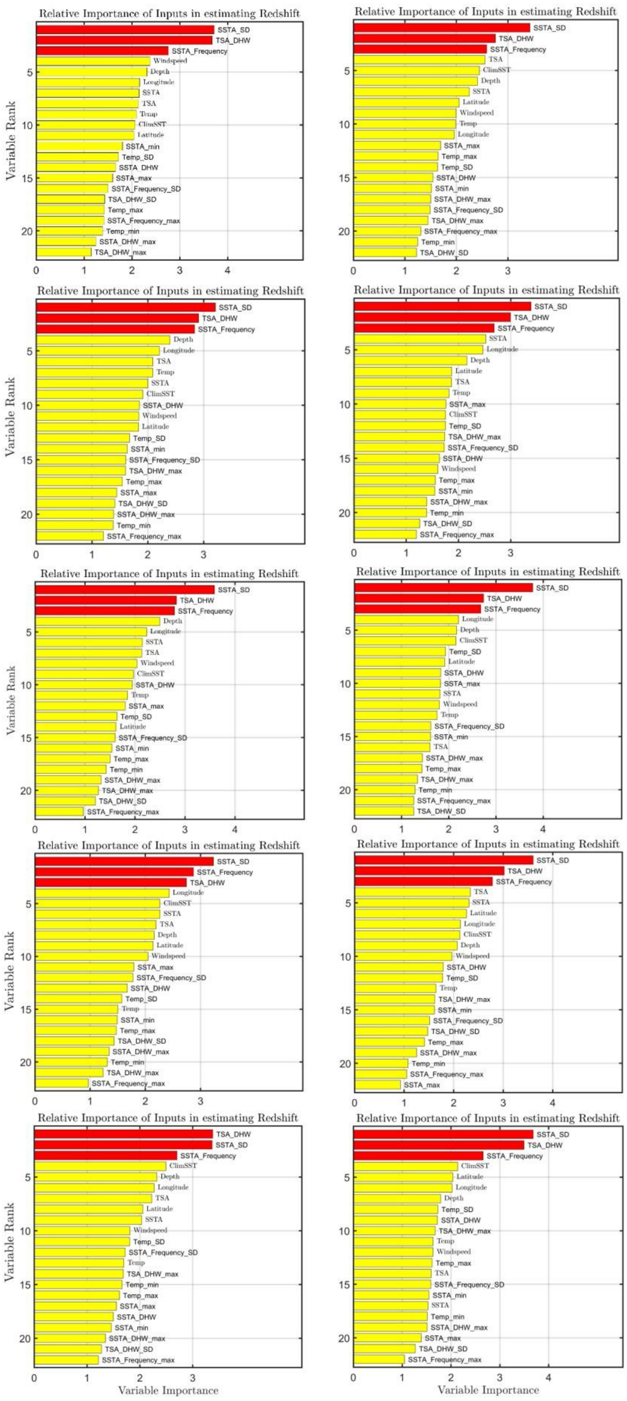

Figure S2. Relative importance assessment of 10 random forest model parameters trained on the global coral-bleaching database. The model's predictive accuracy is recalculated using the shuffled OOB sample. The difference in accuracy before and after shuffling is recorded. The process is repeated across all trees in the forest, and the mean decrease in accuracy is computed. This mean decrease serves as a measure of the variable's importance (I_v), reflecting how crucial the variable is for maintaining predictive accuracy. A substantial decrease in accuracy indicates high importance, while a negligible or negative change suggests that the variable contributes little to the model's predictions. Negative importance scores, which may arise due to random noise, are generally interpreted as zero importance.

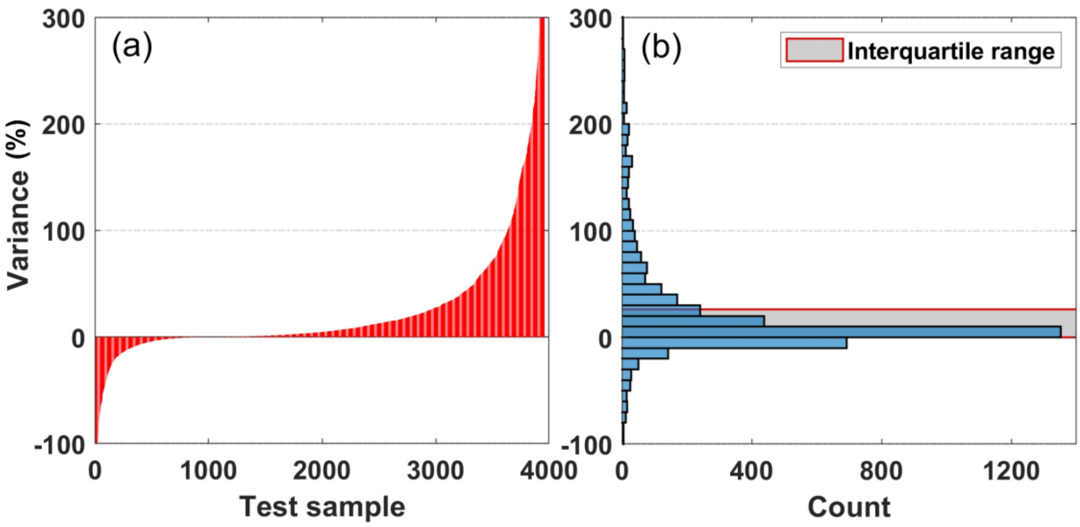

Figure S3. Diagnostic analysis of model uncertainty based on random forest prediction variance. (a) Prediction variance for each test sample derived from the RF ensemble, quantifying individual-level uncertainty. (b) Distribution of prediction variances across all test samples; the interquartile range (IQR) indicates the typical spread of uncertainty, highlighting the proportion of samples with low variance and thus higher prediction confidence.

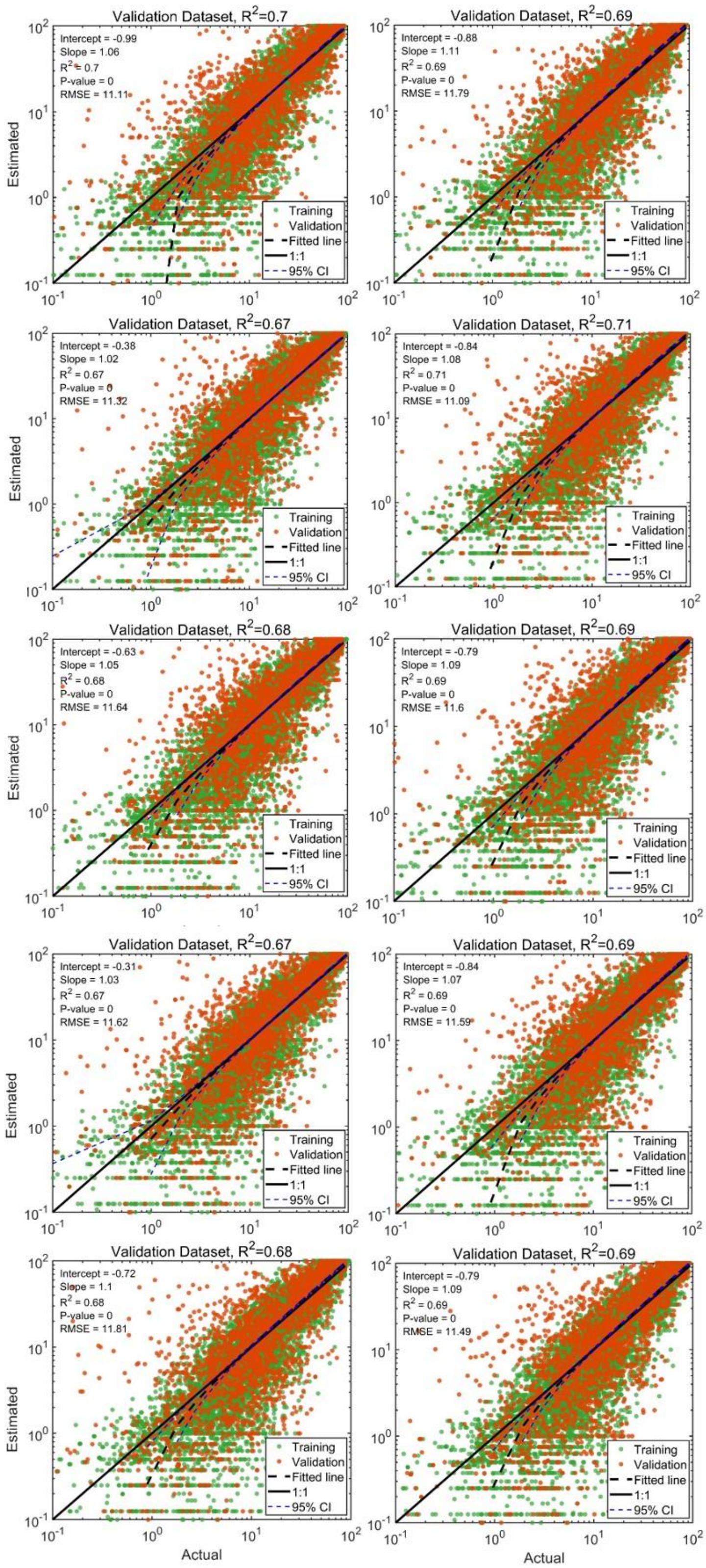

Figure S4. Models of 10 random forest training based on the global coral-bleaching database. To assess model performance and validate its generalization ability, we randomly split the dataset into a training set (80%) and a test set (20%). In addition, we averaged the results of 10 trainings as the final output to avoid the instability of the projection model due to the random selection of the training dataset.

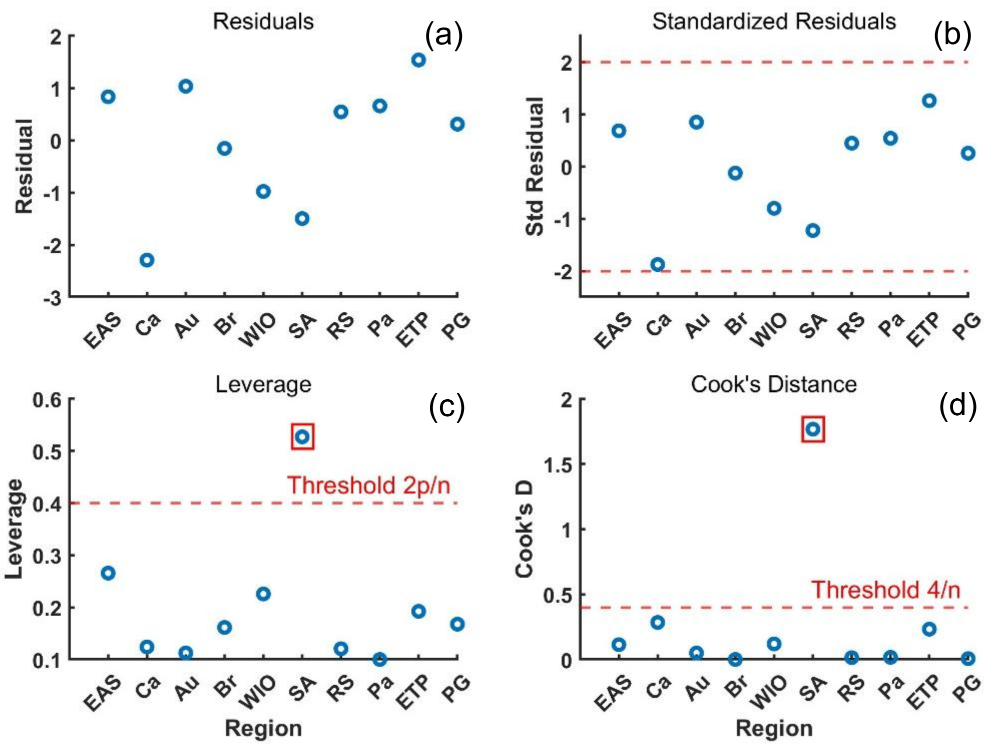

Figure S5. Standard diagnostic plots for the linear regression between coral reef decline rate (%) and bleaching severity across 10 tropical ocean regions. (a) Raw residuals plotted by region reveal deviations from model predictions. (b) Standardized residuals identify potential outliers; values beyond ±2 (dashed red lines) suggest possible concern. (c) Leverage values indicate each observation's influence on model fit; the red dashed line marks the conventional threshold of 2p/n. (d) Cook's Distance highlights influential data points; values above 4/n (dashed red line) are considered potentially influential. South Asia (SA) exceeds multiple thresholds and is flagged as an influential point.

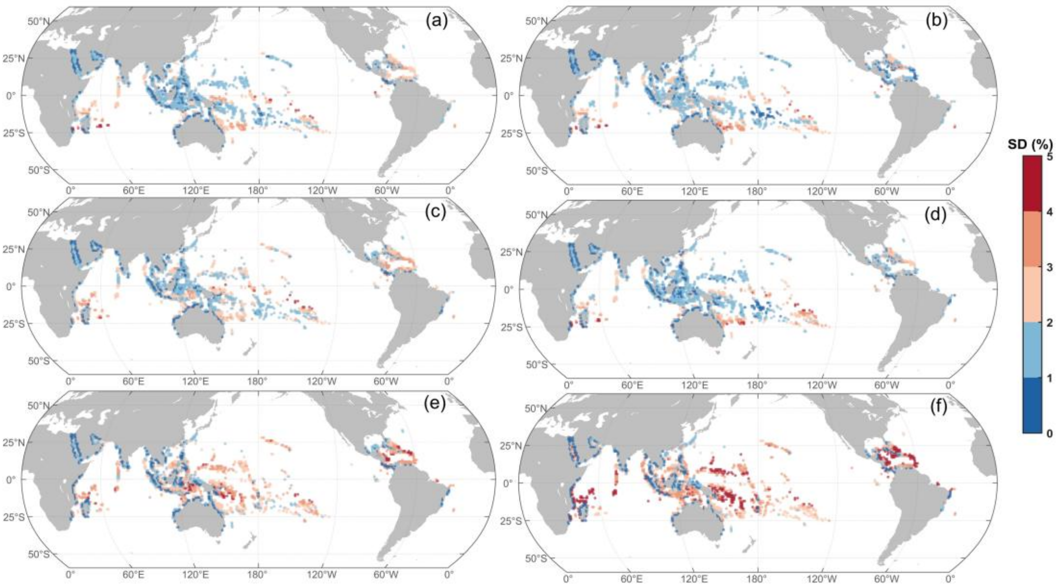

Figure S6. Standard deviation of mean annual coral bleaching projections based on CMIP6 data for the periods 2020–2060 (a, c, and e) and 2060–2100 (b, d, and f), under three climate scenarios: (a, b) low emission (SSP1-2.6), (c, d) medium emission (SSP2-4.5), and (e, f) high emission (SSP5-8.5) during the periods 2020–2060 (a, c, e) and 2060–2100 (b, d, f).

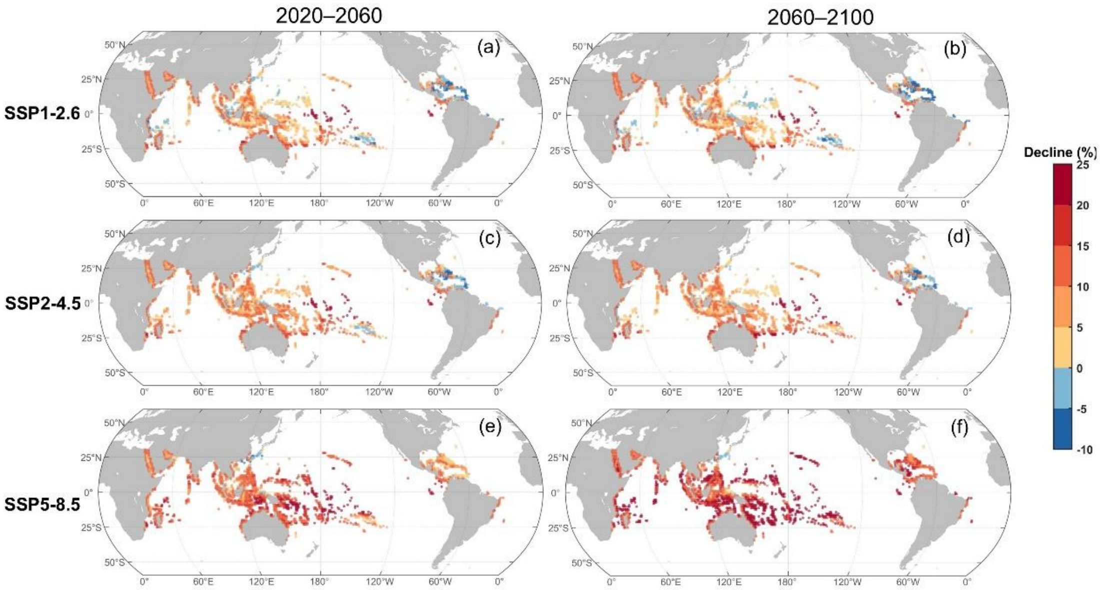

Figure S7. Projected coral decline under three climate scenarios: (a, b) low emission (SSP1-2.6), (c, d) medium emission (SSP2-4.5), and (e, f) high emission (SSP5-8.5) during the periods 2020–2060 (a, c, e) and 2060–2100 (b, d, f).

Supplementary References

Bentsen, Mats; Oliviè, Dirk Jan Leo; Seland, Øyvind; Toniazzo, Thomas; Gjermundsen, Ada; Graff, Lise Seland; Debernard, Jens Boldingh; Gupta, Alok Kumar; He, Yanchun; Kirkevåg, Alf; Schwinger, Jörg; Tjiputra, Jerry; Aas, Kjetil Schanke; Bethke, Ingo; Fan, Yuanchao; Griesfeller, Jan; Grini, Alf; Guo, Chuncheng; Ilicak, Mehmet; Karset, Inger Helene Hafsahl; Landgren, Oskar Andreas; Liakka, Johan; Moseid, Kine Onsum; Nummelin, Aleksi; Spensberger, Clemens; Tang, Hui; Zhang, Zhongshi; Heinze, Christoph; Iversen, Trond; Schulz, Michael (2019). NCC NorESM2-MM model output prepared for CMIP6 ScenarioMIP ssp585. Earth System Grid Federation. https://doi.org/10.22033/ESGF/CMIP6.8321

Boucher, Olivier; Denvil, Sébastien; Levavasseur, Guillaume; Cozic, Anne; Caubel, Arnaud; Foujols, Marie-Alice; Meurdesoif, Yann; Cadule, Patricia; Devilliers, Marion; Dupont, Eliott; Lurton, Thibaut (2019). IPSL IPSL-CM6A-LR model output prepared for CMIP6 ScenarioMIP ssp585. Version YYYYMMDD[1].Earth System Grid Federation. https://doi.org/10.22033/ESGF/CMIP6.5271

Cao, Jian (2019). NUIST NESMv3 model output prepared for CMIP6 ScenarioMIP ssp245. Earth System Grid Federation. https://doi.org/10.22033/ESGF/CMIP6.8781

Danabasoglu, Gokhan (2019). NCAR CESM2-WACCM model output prepared for CMIP6 ScenarioMIP ssp585. Earth System Grid Federation. https://doi.org/10.22033/ESGF/CMIP6.10115

Dix, Martin; Bi, Daohua; Dobrohotoff, Peter; Fiedler, Russell; Harman, Ian; Law, Rachel; Mackallah, Chloe; Marsland, Simon; O'Farrell, Siobhan; Rashid, Harun; Srbinovsky, Jhan; Sullivan, Arnold; Trenham, Claire; Vohralik, Peter; Watterson, Ian; Williams, Gareth; Woodhouse, Matthew; Bodman, Roger; Dias, Fabio Boeira; Domingues, Catia M.; Hannah, Nicholas; Heerdegen, Aidan; Savita, Abhishek; Wales, Scott; Allen, Chris; Druken, Kelsey; Evans, Ben; Richards, Clare; Ridzwan, Syazwan Mohamed; Roberts, Dale; Smillie, Jon; Snow, Kate; Ward, Marshall; Yang, Rui (2019). CSIRO-ARCCSS ACCESS-CM2 model output prepared for CMIP6 ScenarioMIP ssp585. Earth System Grid Federation. https://doi.org/10.22033/ESGF/CMIP6.4332

EC-Earth Consortium (EC-Earth) (2019). EC-Earth-Consortium EC-Earth3 model output prepared for CMIP6 CMIP historical. Earth System Grid Federation. https://doi.org/10.22033/ESGF/CMIP6.4700

EC-Earth Consortium (EC-Earth) (2019). EC-Earth-Consortium EC-Earth3-Veg model output prepared for CMIP6 ScenarioMIP. Earth System Grid Federation. https://doi.org/10.22033/ESGF/CMIP6.727

EC-Earth Consortium (EC-Earth) (2020). EC-Earth-Consortium EC-Earth3-Veg-LR model output prepared for CMIP6 ScenarioMIP ssp119. Earth System Grid Federation. https://doi.org/10.22033/ESGF/CMIP6.4873

Lovato, Tomas; Peano, Daniele (2020). CMCC CMCC-CM2-SR5 model output prepared for CMIP6 ScenarioMIP ssp585. Earth System Grid Federation. https://doi.org/10.22033/ESGF/CMIP6.3896

Lovato, Tomas; Peano, Daniele; Butenschön, Momme (2021). CMCC CMCC-ESM2 model output prepared for CMIP6 CMIP historical. Earth System Grid Federation.

https://doi.org/10.22033/ESGF/CMIP6.13195

Schupfner, Martin; Wieners, Karl-Hermann; Wachsmann, Fabian; Steger, Christian; Bittner, Matthias; Jungclaus, Johann; Früh, Barbara; Pankatz, Klaus; Giorgetta, Marco; Reick, Christian; Legutke, Stephanie; Esch, Monika; Gayler, Veronika; Haak, Helmuth; de Vrese, Philipp; Raddatz, Thomas; Mauritsen, Thorsten; von Storch, Jin-Song; Behrens, Jörg; Brovkin, Victor; Claussen, Martin; Crueger, Traute; Fast, Irina; Fiedler, Stephanie; Hagemann, Stefan; Hohenegger, Cathy; Jahns, Thomas; Kloster, Silvia; Kinne, Stefan; Lasslop, Gitta; Kornblueh, Luis; Marotzke, Jochem; Matei, Daniela; Meraner, Katharina; Mikolajewicz, Uwe; Modali, Kameswarrao; Mü ller, Wolfgang; Nabel, Julia; Notz, Dirk; Peters-von Gehlen, Karsten; Pincus, Robert; Pohlmann, Holger; Pongratz, Julia; Rast, Sebastian; Schmidt, Hauke; Schnur, Reiner; Schulzweida, Uwe; Six, Katharina; Stevens, Bjorn; Voigt, Aiko; Roeckner, Erich (2019). DKRZ MPI-ESM1.2-HR model output prepared for CMIP6 ScenarioMIP ssp585. Earth System Grid Federation. https://doi.org/10.22033/ESGF/CMIP6.4403

Seland, Øyvind; Bentsen, Mats; Oliviè, Dirk Jan Leo; Toniazzo, Thomas; Gjermundsen, Ada; Graff, Lise Seland; Debernard, Jens Boldingh; Gupta, Alok Kumar; He, Yanchun; Kirkevåg, Alf; Schwinger, Jörg; Tjiputra, Jerry; Aas, Kjetil Schanke; Bethke, Ingo; Fan, Yuanchao; Griesfeller, Jan; Grini, Alf; Guo, Chuncheng; Ilicak, Mehmet; Karset, Inger Helene Hafsahl; Landgren, Oskar Andreas; Liakka, Johan; Moseid, Kine Onsum; Nummelin, Aleksi; Spensberger, Clemens; Tang, Hui; Zhang, Zhongshi; Heinze, Christoph; Iversen, Trond; Schulz, Michael (2019). NCC NorESM2-LM model output prepared for CMIP6 ScenarioMIP ssp585. Earth System Grid Federation. https://doi.org/10.22033/ESGF/CMIP6.8319

Swart, Neil Cameron; Cole, Jason N.S.; Kharin, Viatcheslav V.; Lazare, Mike; Scinocca, John F.; Gillett, Nathan P.; Anstey, James; Arora, Vivek; Christian, James R.; Jiao, Yanjun; Lee, Warren G.; Majaess, Fouad; Saenko, Oleg A.; Seiler, Christian; Seinen, Clint; Shao, Andrew; Solheim, Larry; von Salzen, Knut; Yang, Duo; Winter, Barbara; Sigmond, Michael (2019). CCCma CanESM5-CanOE model output prepared for CMIP6 ScenarioMIP ssp585. Earth System Grid Federation. https://doi.org/10.22033/ESGF/CMIP6.10276

van Woesik, R. & Kratochwill, C. A global coral-bleaching database, 1980–2020. *Scientific Data* **9**, 20 (2022). https://doi.org/10.1038/s41597-022-01121-y

Xin, Xiaoge; Wu, Tongwen; Shi, Xueli; Zhang, Fang; Li, Jianglong; Chu, Min; Liu, Qianxia; Yan, Jinghui; Ma, Qiang; Wei, Min (2019). BCC BCC-CSM2MR model output prepared for CMIP6 ScenarioMIP ssp585. Earth System Grid Federation. https://doi.org/10.22033/ESGF/CMIP6.3050

Yukimoto, Seiji; Koshiro, Tsuyoshi; Kawai, Hideaki; Oshima, Naga; Yoshida, Kohei; Urakawa, Shogo; Tsujino, Hiroyuki; Deushi, Makoto; Tanaka, Taichu; Hosaka, Masahiro; Yoshimura, Hiromasa; Shindo, Eiki; Mizuta, Ryo; Ishii, Masayoshi; Obata, Atsushi; Adachi, Yukimasa (2019). MRI MRI-ESM2.0 model output prepared for CMIP6 ScenarioMIP ssp585. Earth System Grid Federation. https://doi.org/10.22033/ESGF/CMIP6.6929

Ziehn, Tilo; Chamberlain, Matthew; Lenton, Andrew; Law, Rachel; Bodman, Roger; Dix, Martin; Wang, Yingping; Dobrohotoff, Peter; Srbinovsky, Jhan; Stevens, Lauren; Vohralik, Peter; Mackallah, Chloe; Sullivan, Arnold; O'Farrell, Siobhan; Druken, Kelsey (2019). CSIRO ACCESS-ESM1.5 model output prepared for CMIP6 ScenarioMIP ssp585. Version YYYYMMDD[1].Earth System Grid Federation. https://doi.org/10.22033/ESGF/CMIP6.4333